Imaging Interferometers Using Flat Primary Segments

E. M. Sabatke and J. H. Burge
Optical Sciences Center
University of Arizona
1630 East University Boulevard
Tucson, AZ 85721

ABSTRACT

Gossamer mirrors have the potential to reach 100 meter baselines in space because of their very light weight. We explore a type of system that uses an array of flat gossamer mirrors as a primary mirror. Using wavefront reconstruction, we can easily estimate the fields of view for these systems. We report the fields of view as a function of the free parameters for these systems.

Keywords: imaging interferometers, telescope design, multiple aperture systems

1. INTRODUCTION

Baselines of 100 meters are needed in future space telescopes in order to image extra-solar planets directly. To achieve this, optics are needed that are orders of magnitude lighter and larger than those currently in use. Since rocket shrouds currently limit optics to four meters in diameter, the optics will certainly need to be segmented.

Our research group is developing a flat membrane technology, and I have looked at one type of telescope design that uses such flat membrane mirrors. The concept is sketched in Figure 1. The primary is an array of flat gossamer segments, and is free-flying with respect to the rest of the system. The segmented primary then has a low power, making the effects of the segmentation less noticeable. In space, there is no compelling reason to make systems as short as possible, so such weak systems with better performance than fast ones are allowed. Each primary segment points to a single, shared secondary.

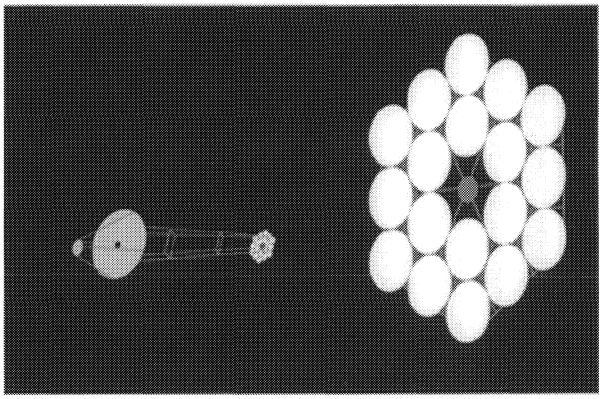

Figure 1: A space telescope concept. The primary is an array of flat gossamer mirrors.

The tertiary is also an array, with one mirror corresponding to one primary flat, and handling only the beam from that flat. To ease the tolerances on the primary mirror, the secondary power is chosen so that it images the primary array onto the tertiary array. If these tertiaries have tip/tilt/piston control, they can be

used to compensate for position shifts of the primary segments. In this way, the mechanical structure that supports the primary flats doesn't have to be excessively rigid, and can have a relatively low mass.

2. FIVE-FLAT SYSTEM GEOMETRY

To explore this idea more quantitatively, I used a system of five flats arranged in a "+" configuration, as shown in Figure 2. I defined the systems in terms of the four possible degrees of freedom: L is the length of the system, M is the demagnification due to the secondary, D is the diameter of a single primary flat, and C is the distance of the center flat from the system axis. These parameters are shown in a side view of the five-flat system in Figure 3.

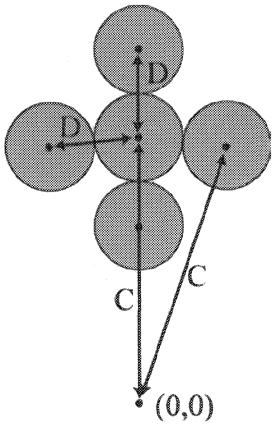

Figure 2: A primary array of five flat mirrors, shifted off-axis by C and with flats separated by D.

The "power" of the primary array is L, so that all the flats focus onto the center of the secondary. The secondary power images the primary onto the tertiary array. The image plane is assumed to be directly behind the secondary mirror, and so the powers of the tertiaries are chosen so that the image location is the image plane. Since the beams from the primaries fall on the secondary at an angle, they leave the secondary with significant astigmatism even for zero field angles. The tertiaries have different radii of curvature in the x and y directions, in order to compensate for this astigmatism.

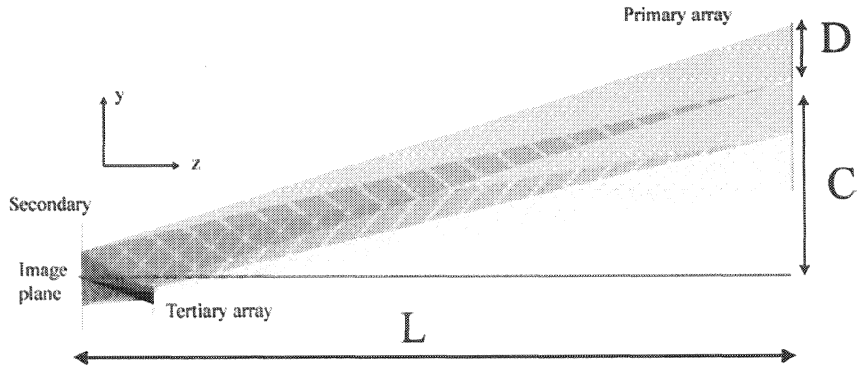

Figure 3: A side view of the five-flat systems, with the system parameters shown. (The drawing has been compressed along the z-axis.)

3. COMBINING ISSUES

The individual branches of these systems are quite slow, so combining errors limit the field of view rather than errors in the individual arms. A perfect point spread function from the five-flat system is shown in Figure 4. The total image is made up of the individual images from each branch of the system, and sets of fringes from each pair of branches in the system. All of these images and fringe centers must coincide, and they must coincide as a function of field, as well as at zero field angles.

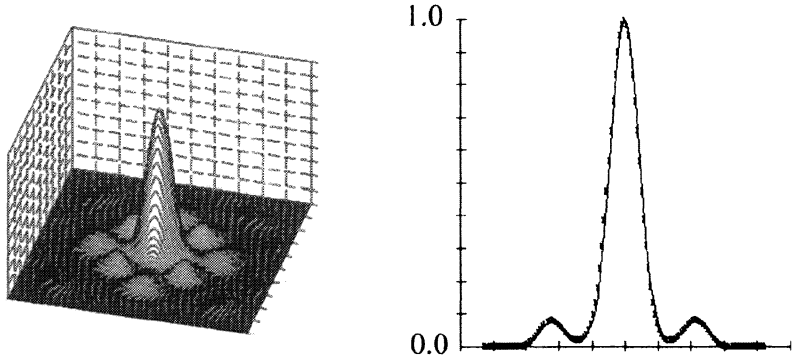

Figure 4: Unaberrated PSF from a five-flat gossamer system, 3D surface and a cross-section.

A variety of things can go wrong. It makes sense to address the problems that have the lowest orders in field angle first. At zero field angle, the images from each branch must overlap in the x-y plane. This sets the pointing for each branch of the system. The images must also overlap in the z-direction, so this requires that there be no defocus errors between the branches. And finally, the fringe centers must coincide with the images, so the pathlengths of the axial rays in each branch must all be equal. All of these conditions are easily satisfied in the five-flat systems.

Next, problems that are linear with field angle can appear.

3.1. Linear piston errors

Piston errors are a mismatch in the optical pathlengths between two branches of the system, and cause the fringe centers to move away from the individual images. Piston errors that are linear with field angle can be corrected by satisfying the Abbe sine condition for the axial rays in each branch. The Abbe sine condition is well known for eliminating coma in single aperture systems (provided the spherical has already been corrected). It is easy to see from Figure 5 that if the continuous coma wavefront were "sampled" by a multiple aperture system, there would be an apparent phase error between the two apertures. Since coma is linear with field angle, the phase error would increase linearly with field, as well. Since the Abbe sine condition eliminates coma, satisfying the Abbe sine condition for the axial rays in each branch would eliminate the linear piston in a multiple aperture system. It is not necessary to satisfy the Abbe sine condition for the entire wavefront, when linear piston errors are the concern.

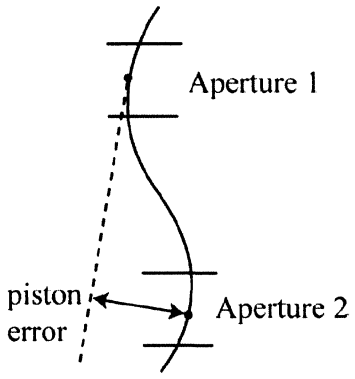

Figure 5: Linear phase errors in a multiple aperture system can be interpreted as coma. Satisfying the Abbe sine condition for the rays at the center of each aperture, then, eliminates the linear piston errors.

For an afocal system, the Abbe sine condition has the form $h / \sin\theta = K$, where K is a constant over all values of h. The variables are shown in Figure 6. The height of a ray into the system is h, and θ is that ray's angle in object space. Only rays at zero field angle need to be considered.

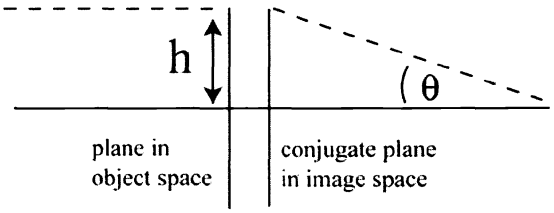

Figure 6: The afocal sine condition requires that $h / \sin\theta = K$, for all h. This corrects coma at all field angles, in the absence of spherical aberration.

In the five-flat systems, the Abbe sine condition was satisfied for the axial rays using simple geometry. As shown in Figure 7, the ray angle of an axial ray in image space is equal to the ray angle after reflection from the primaries. The axial rays enter the system at the center of each primary, and so the values of h that need to be considered are C+D,C, and C-D. If each primary is located on a sphere of radius L, then K = L for each of these axial rays, the sine condition is satisfied, and the linear piston errors are eliminated.

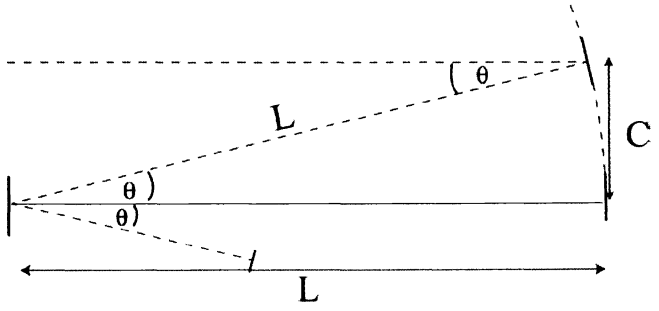

Figure 7: The axial ray angle in image space is equal to the ray angle after reflection from the primary. Satisfying the sine condition for the axial rays then requires that the primary flats lie on a sphere of radius L.

3.2. Linear tilt and power errors

Tilt errors cause the images to separate in their x and y coordinates, and power errors can be thought of as image separation in the z-coordinate. The linear tilt and power errors could not be corrected for these systems, but were minimized.

In theory, if the image planes for each branch of the system coincided, and all the branches had the same focal length, then the each image would move by ($f\alpha$) for a field angle of α. The images would stay together as a function of field.

In the five-flat systems, the image planes for each individual branch are physically tilted in space. The situation is shown in Figure 8. The amount the image plane is tilted is determined by the Scheimpflug condition,[1] which states that the object and image planes will intersect over a system's principle planes. Because of the slanted image planes, the images separate as a function of field. In addition, a defocus that is linear in field is introduced, because the individual image planes separate in space for non-zero field angles.

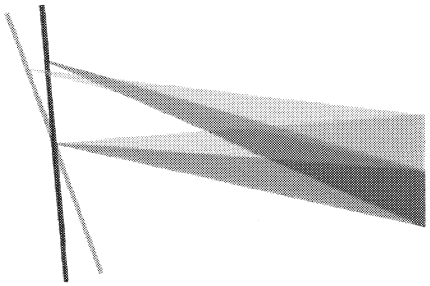

Figure 8: The image planes from each branch are tilted with respect to one another. This introduces both tilt and defocus errors that are linear with field angle. Two beams are shown for a zero field angle and a non-zero field angle.

In a system with more degrees of freedom, an off-axis mirror could be used to correct for the tilted image planes, but this is not possible in the five-flat systems. It is also not desirable to force the focal lengths of each branch to match in these systems. The focal lengths could be made equal by adjusting the tertiary powers (the secondary is shared, so its power can't affect this, and the primary has no power). Adjusting the tertiary powers, though, introduces large defocus errors that are constant with field angle. Those defocus errors are worse than the tilt errors that would be partially corrected by matching focal lengths.

3.3. Estimating the fields of view

The tilt and defocus errors that couldn't be corrected gave an easy way to estimate the fields of view of these systems. Those errors will dominate for small field angles, and can be calculated geometrically. One can then convert the geometric distances to wavefront errors, and reconstruct the wavefront. Finally, one can calculate the RMS wavefront error, which gives a good estimate of the FOV for the system. This is discussed in detail in other sources.[2] After confirming this estimate for several systems with a full raytrace model, I used it to quickly explore a wide range of systems.

4. EXPLORING PARAMETER SPACE

I used the wavefront reconstruction method to explore the parameter space of the five-flat systems. (The parameters are shown in Figure 3.) There are four parameters, so I chose to sample three values from each, giving a total of 81 data points. I tried to select reasonable values for each parameter, and those values are shown below.

D	primary flat diameter	1 m	2 m	5 m
M	magnification of secondary	0.2	0.1	0.05

L	length of the system	1000 m	750 m	500 m
C	center flat's distance off-axis	15 m	30 m	50 m

The flat diameters are limited by the tertiary diameters, as well as fabrication techniques and rocket shroud sizes. The tertiary mirrors are traditional glass mirrors, and must be small and easy to handle. I assumed that the largest acceptable tertiary would be 1 meter in diameter. For the magnifications I selected, this limits the flat diameters to 5 meters or less. Longer system lengths mean better performance, and 1 km seems to be the largest system we can conceive of controlling at this time. I chose a maximum off-axis distance for the center primary, C, of 50 meters, since this would mean a 100 meter baseline if the system were used as a pair with another, identical system. The systems with the best performance, then, will have the parameter values shown in the first column of the table - the smallest flat diameters, largest magnification, longest length, and shortest distance off-axis.

5. RESULTS AND CONCLUSIONS

The fields of view for the systems are shown in Figure 9. It is difficult to represent four-dimensional space in a useful way, but the plots below contain all 81 data points considered. As expected, the FOV improves with decreasing flat diameters and increasing system lengths. It also improves with decreasing magnification and decreasing primary heights. The fields of view were most sensitive to the magnification parameter.

The best system (D = 1 m, M = 0.2, L = 1000 m, C = 15 m) had a FOV of 1.3 degrees. One-meter flats give a total collection area of only 15.7 square meters. The best system with an off-axis distance of 50 meters had a FOV of 0.36 degrees. The fastest system considered (D = 5 m, M = 0.05, L = 500 m, C = 50 m) had a field of view of 1.2 arcsec.

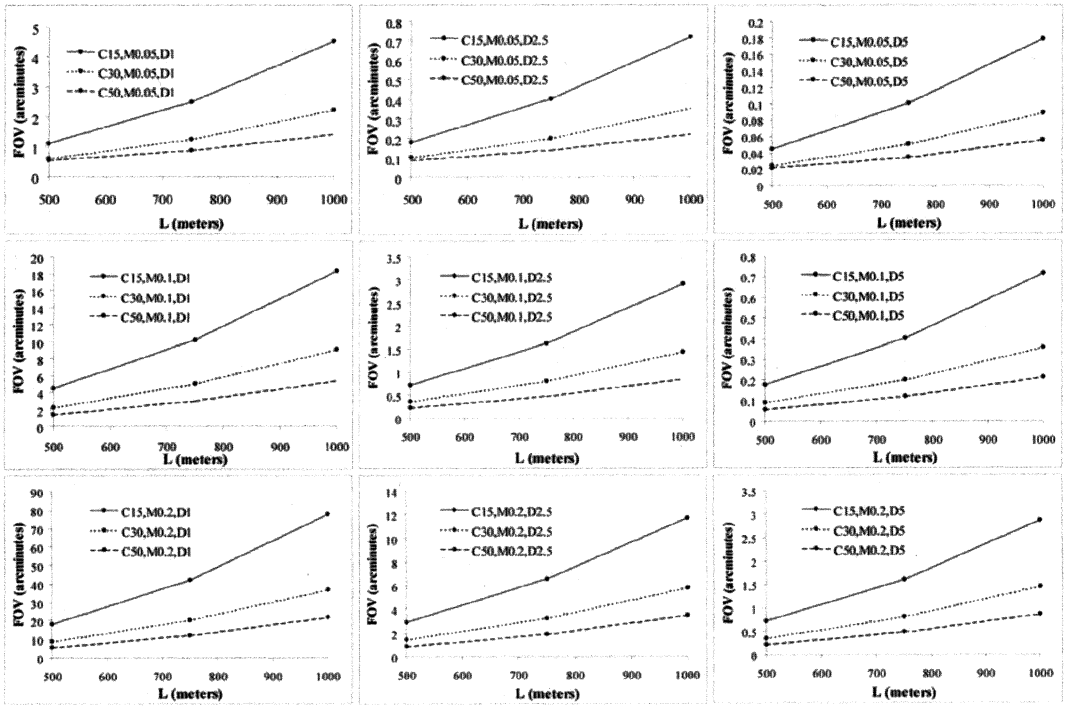

Figure 9: Fields of view for the five-flat gossamer systems studied. Plots are FOV vs. L, the system length. Off-axis distance C is a parameter in the plots. Magnification M decreases across the rows, and flat diameter D increases down

the columns.

REFERENCES

1. R. N. Wilson, Reflecting Telescope Optics I: Basic Design Theory and its Historical Development (Springer-Verlag, New York, 1996), p. 82-83.
2. E. M. Sabatke and J. H. Burge, "Basic Principles in the optical design of imaging multiple aperture systems," in International Optical Design Conference 2002, J. Sasian and P. K. Manhart, ed., *Proc. SPIE* **4832**, 2002.